Available online at www.sciencedirect.com

SciVerse ScienceDirect

Physics Procedia 40 (2013) 38 – 44

Physics Procedia

2nd European Conference on Nano Films: ECNF-2012

Influence of heat treatments on the structure of FeAl powders mixture obtained by mechanical alloying

Mohsen Mhadhbi[a*], Joan Josep Suñol[b], Mohamed Khitouni[c]

[a] *Laboratory of Useful Materials, National Institute of Research and Physicochemical Analysis, Technopol of Sidi Thabet 2020, Tunisia*

[b] *Department of Physics, University of Girona, Campus Montilivi, Girona 17071, Spain*

[c] *Laboratory of Inorganic Chemistry, 99/UR/12-22, Sciences Faculty of Sfax, Sfax 3018, Tunisia*

Abstract

A nanocrystalline Fe(Al) solid solution was prepared by mechanical alloying (MA) of Fe and Al elemental powders using a planetary ball mill under argon atmosphere. The powder milled for 20 h was annealed at 250, 550 and 650 °C for 1 h. The phase transformations and structural changes occurring in the studied material during mechanical alloying and during subsequent annealing were investigated by X-ray diffraction. The morphology of the powders after MA was examined via SEM and TEM.

Keywords: Mechanical alloying; X-ray diffraction; TEM analysis; FeAl powders; Annealing

1. Introduction

Mechanical alloying (MA) is a powder processing technique that allows production of homogeneous materials starting from blended elemental powder mixtures [1]. Now, it has been shown to be capable of synthesizing a variety of equilibrium and non-equilibrium alloy phases starting from blended elemental or prealloyed powders.

FeAl-based alloys have drawn much attention as materials for high temperature applications because they are low cost intermetallic materials with a relatively low density (5.56 g/cm^3) and exhibit good mechanical properties, and excellent corrosion resistance in oxidizing and sulfidizing atmospheres, which are relied on their ability to form a highly protective Al_2O_3 scale [2-5]. These features make the FeAl

* Corresponding author. Tel.: +21671537666; fax: +21671537688.
E-mail address: mohsen.mhadhbi@inrap.rnrt.tn.

doi:10.1016/j.phpro.2012.12.005

intermetallic compound a very attractive material for structural and coatings applications at elevated temperatures in hostile environments [6]. Recently, it has been show that the heat treatment at 500 ºC results in the complete transformation of Fe(Al) solid solution to FeAl intermetallic compound [7]. Varin et al. [8] are studied the effects of annealing on the microstructure and microhardness of Fe-45at.%Al powders. The phase transformations and structural changes occurring during mechanical alloying of the Fe–50% Al (at.%) powder mixture and during subsequent heating are studied by Krasnowski et al. [9]. Recently, it has been shown that the relative LRO parameter, *S*, of the annealed Fe-45 at.% Al nanopowders, obtained by ball milling, is restored to the level of 0.8-0.9 rather than 1.0, suggest that the powders annealed at 600 ºC retain some residual antisite-atom pairs after annealing [8]. Partially ordered FeAl phase by mechanical alloying of Fe–50 at.%Al powder mixture is also reported [10]. An additional heat treatment is required after the milling to form the fully ordered structure. According to the Fe–Al phase diagram, the ordered bcc or B2 phase exists over the composition range 36–50 at.% Al at room temperature [11, 12].

The intention of this work is to investigate the effects of annealing on the microstructural evolution of FeAl powders obtained by mechanical alloying.

2. Experimental

Elemental powders of Fe (99.9 % purity) and Al (99.3 % purity) with a nominal composition of Fe-40at.%Al were mechanically alloyed in a planetary ball mill (Fritsch Pulverisette 7) to 20 h under argon atmosphere. The milling time is devised to avoid the increasing of temperature inner the container. X-ray diffraction profile for each sample was recorded from the mechanical alloying and annealed powders using Siemens D5000 X-ray diffractometer with Cu K_α radiation. The time spent for collecting data per step was 4 s. Microstructural parameters were calculated, from XRD data, by using Halder–Wagner method [13]. The instrumental broadening was determined using Si standard and subtracted from the experimental breadth to obtain the physical broadening of each diffraction line. For the phase analysis, X'Pert High Score plus program was used. The samples were observed under the transmission electron microscopy (TEM) Philips G20 Ultra-Twin for high resolution equipped. TEM observations were used to confirm the nanocrystallite size obtained by XRD. The morphology of the MA and annealed powders was analyzed by scanning electron microscopy JEOL, model JSM-5200.

3. Results and discussion

3.1. Mechanical alloying of FeAl powders

Fig. 1 shows the 3D XRD patterns of the Fe-40at.%Al powders as a function of milling time. After MA for 12 h, we can see that the intensity of the most intense Al (111) peak is very low. Moreover, the free of overlapping Al (311) peak is not present. Therefore, we can assume that the contribution of other relatively less intense Al peaks to the intensity of the asymmetric peaks is negligible. This allows us to fit and analyse all the asymmetric peaks in the XRD pattern of the powder mechanically alloyed for 12 h. After 14 h of milling, the Al (111) peak disappears completely whereas the remaining peaks become more symmetric (i.e. the b.c.c. (211) peak) and the X-ray peaks move to slightly lower angles. This suggests that a Fe(Al) solid solution is formed by replacement of the separate Fe and Al phases [14]. The XRD patterns of the powders mechanically alloyed for 16, 18 and 20 h do not differ from the pattern obtained

after 14 h of milling. No superlattice peaks corresponding to B2 ordering were observed in these MA powders.

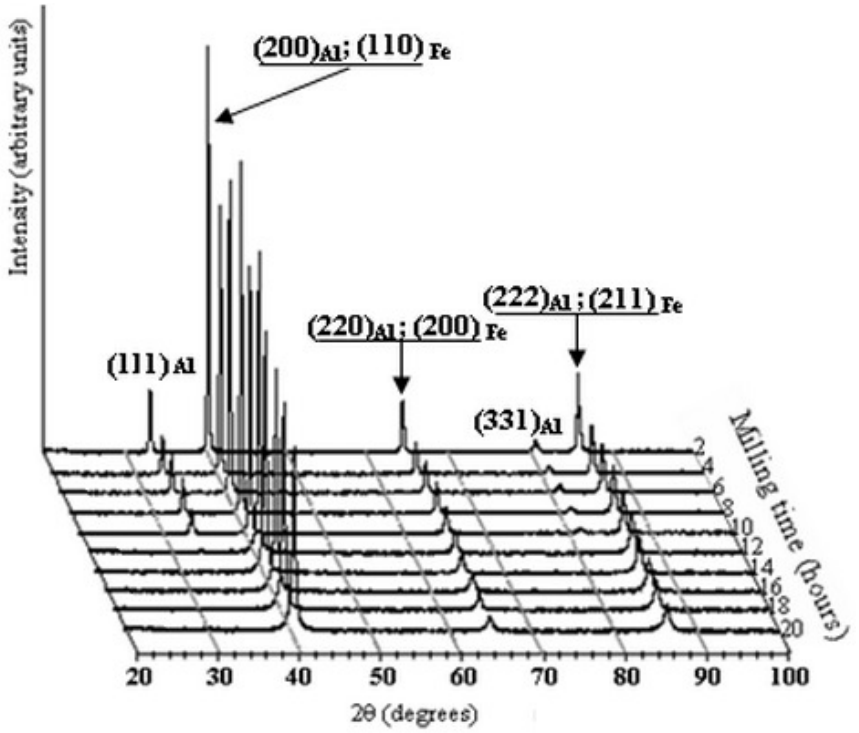

Fig. 1 XRD patterns of the Fe-40at.%Al powders as a function of milling time.

TEM micrographs of the FeAl powders MA for 2 and 20 h are shown in Fig. 2. The crystallite size, measured by TEM, is less than 100 nm (about 63 nm) that is in good agreement with the value determined from XRD (Fig. 2a). In fact, crystallite size measured by TEM (about 70 nm) is consistent with those measured by X-ray diffraction. The MA material assumes a flake-like irregular morphology with zones of pure aluminum and iron. This result is similar to these obtained by Valdrè et al. [15]. In addition, some contrasts of parallel-array of fringes are also visible. This defect results from the plastic deformation introduced during high energy mechanical milling. Electron diffraction patterns (Fig. 1b) still show both reflections from the b.c.c. α-iron and f.c.c. aluminum structures (Fig. 2b). The bright-field TEM image of the FeAl powders after 20 h of MA is shown in Fig. 2c. It can be seen that the powder particles have a greater agglomeration. This may be a result of the welding of particles powder occurring during MA after long times of milling and the high density of dislocation. The electron diffraction pattern shows in Fig. 2d indicating the Al solid-solution in the host b.c.c. Fe lattice when the (110), (200), (211), (220) and (221) rings are clearly visible. They represent the diffraction of the fundamental lattice planes of the FeAl structure (b.c.c.).

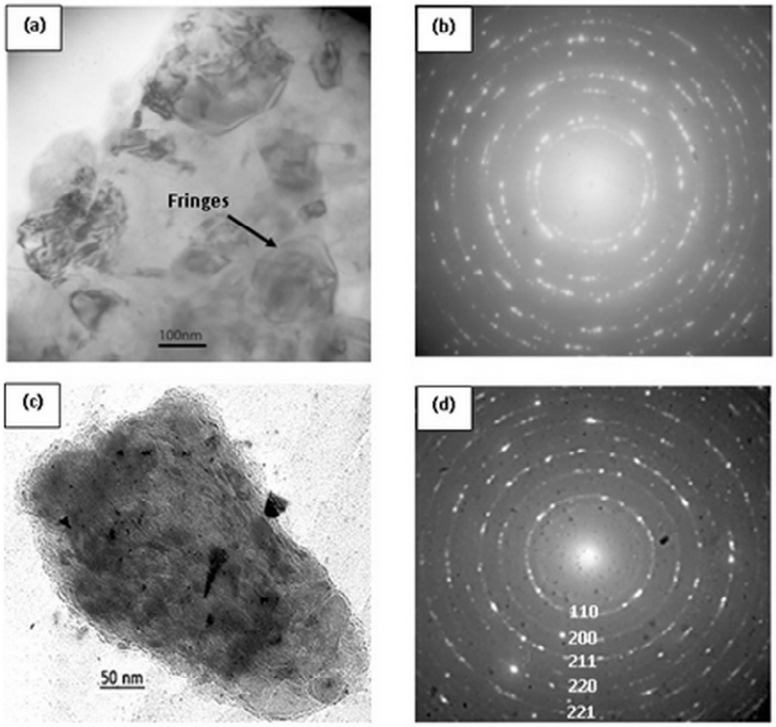

Fig. 2. The bright-field TEM images and electron diffraction patterns of FeAl powders (a, b) MA for 2 h; (c, d) MA for 20 h.

The structural analysis of MA Fe-40at.%Al powders measured by XRD and TEM are illustrate in Table 1. It is clear that increasing of MA time resulted in increasing of microstrain from 0.407 % after 2 h of MA to 1.85 % after 20 h of MA. In addition, the crystallite size deduced by X-ray diffraction decreases with increasing milling time to reach 8 nm after 20 h of MA. The crystallite size of the same sample measured by TEM is equal to 10 nm. These confirm that crystallite sizes measured by TEM are consistent with those measured by XRD.

Table 1. Structural analysis of MA FeAl powders.

Analysis method	FeAl powders MA for 2 h	FeAl powders MA for 20 h
XRD micro-strain (%)	0.407	1.85
XRD crystallite size (nm)	63	8
Tem crystallite size (nm)	70	10

3.2. Annealing of MA FeAl powders

Fig. 3 shows SEM images of the FeAl powders MA for 20 h and annealed at 650 °C. After milling for 20 h, the fine powder tends to form a matrix of randomly welded thin layers of highly deformed particles (Fig. 3a). For the annealed powders (Fig. 3b) ultrafine grains are appearing. Their average size is probably due to the dynamically recrystallized ones observed in the as-milled powders. However, the ultrafine grains formation after annealing is the result of static recrystallization and/or nanocrystalline grain growth processes [8].

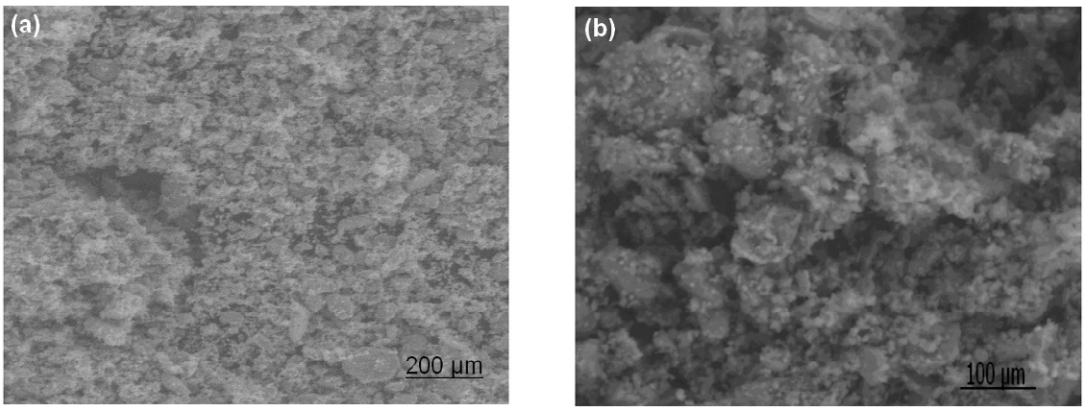

Fig. 3. SEM micrographs of MA FeAl powders (a) MA for 20 h; (b) Annealed at 650 °C.

Fig. 4 shows the XRD patterns of the powders MA for 20 h and annealed for 1 h at 250, 550 and 650 °C. The X-ray diffraction patterns of the Fe(Al) powders annealed at 250 °C do not change significantly compared to the as-milled powders, except for a progressive narrowing and slight shift of the diffraction peaks. Further heating to 550 °C enabled supersaturated Fe(Al) solid solution to precipitate out fine metastable Al_5Fe_2 phase (space group: Cmcm; a = 7.6486 Å, b = 6.4131 Å and c = 4.2165 Å [16]) and fine metastable $Al_{13}Fe_4$ phase (space group: Bmmm; a = 7.7510 Å, b = 4.0336 Å and c = 23.7710 Å [17]). The reason for preferred formation of metastable Fe_2Al_5 and $Al_{13}Fe_4$ intermetallics can be attributed to the non equilibrium nature of MA and also to the lower enthalpies of formation of Fe_2Al_5 in comparison to that of other intermetallics [18]. There is no significant difference between the XRD patterns of the powders being annealed at 550 °C and at 650 °C.

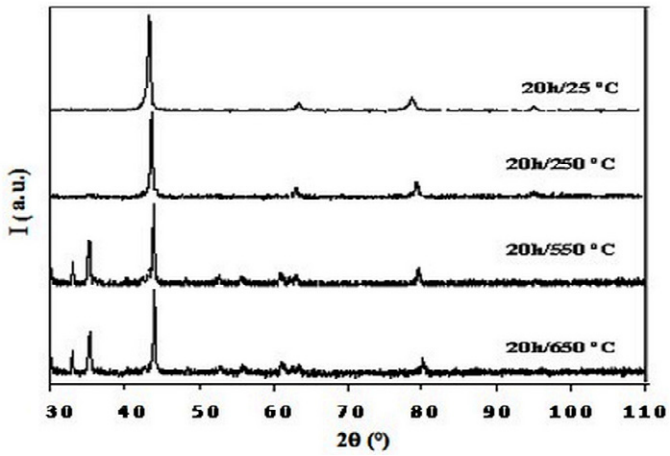

Fig. 4. XRD patterns of FeAl powders MA for 20 h and annealed at various temperatures during 1 h.

The evolution of microstructural properties of FeAl powders MA for 20 h and annealed for 1 h at 250, 550 and 650 °C are presented in Table 2. Annealing causes a decrease in the microstrain and lattice parameter from 1.85 % and 0.291 nm (at 25 °C) to 0.18 % and 0.285 nm (at 650 °C), respectively, and an increase in the crystallite size from 8 nm (at 25°C) to 35 nm (at 650 °C). MA produces lattice defects, especially a high concentration of vacancies in this material. During annealing, movements of the excess vacancies in the lattice lead to the reordering of the structure and the decrease of the number of lattice defects, particularly in highly disordered regions [19]. This result reduces of the microstrain. On the other hand, Fu [20] has shown, from a local-density-functional study, that the size effect is inadequate for explaining the defect structure. Subsequently, by increasing the annealing temperature, the migration distances become larger and these excess vacancies get lost at grain boundaries or dislocation sinks which were produced during MA. This diffusion allows further ordering and a reduction in lattice parameter and microstrain [21]. Higher annealing temperature causes grain growth, since recovery and recrystallization processes occur faster and more time was available for grain growth [22].

Table 2. Evolution of microstructural properties of the MA and heat treated FeAl powders as a function of annealing temperatures.

Alloy	D (nm) ± 2	ε (%)±10^{-2}	a (nm)±10^{-2}
MA for 20 h	8	1.85	0.291
MA for 20 h + annealed at 250 °C	10	0.9	0.290
MA for 20 h + annealed at 550 °C	22	0.3	0.280
MA for 20 h + annealed at 650 °C	35	0.18	0.285

4. Conclusions

In the present study we are study, using essentially TEM and XRD, the microstructural evolution of $Fe_{60}Al_{40}$ powders produced by MA and after annealing. The TEM micrograph and corresponding selected area diffraction (SAD) pattern of the powders MA for 20 h confirming the validity of the XRD analysis in the crystallite size determination. It was found that the nanoscale crystallite size is retained after annealing. During annealing, the crystallite size increased and the lattice parameter and strain decreased and we are noted the formation of both Fe2Al5 and Al13Fe4 intermetallics phases at higher temperature.

Acknowledgements

Financial support from MICYT MAT2006-13925-C02-02 (FEDER) project is acknowledged.

References

[1] Suryanarayana C. *Prog Mater Sci* 2001;**45**:461–484.
[2] Sikka VK, Mavity JT, Anderson K. *Mater Sci Eng A* 1992;**153**:712–721.
[3] Koch CC. *Mater Sci Eng A* 1998;**244**:39–48.
[4] Mitchell TE, Hirth JP, Misra A. *Acta Mater* 2002;**50**:1087–1093.
[5] Stoloff NS. *Mater Sci Eng A*1998; **258**:1–14.
[6] Deevi SC, Sikka VK, Liu CT. *Prog Mat Sci* 1997;**42**:177–192.
[7] Wang T, Li J, Yang J, Li X, Zhang Q, Li Y. *Therm J Spray Technol* 2007;**16**: 669–676.
[8] Varin RA, Bystrzycki J, Calka A. *Intermetallics* 1999;**7**: 917–930.
[9] Krasnowski M, Grabias A, Kulik T. *J Alloys Compd* 2006;**424**: 119–127.
[10] Morris-Munoz MA, Dodge A, Morris DG. *NanoStruct Mater* 1999;**11**: 873–885.
[11] Besnus MJ, Herr A, Meyer A. *J Phys F*: *Metal Phys* 1975;**5**: 2138–2147.
[12] Hernando A, Amils X, Nogues J, Surinach S, Baro MD, Ibarra MR. *Phys Rev B* 1998;**58**: 11864–11870.
[13] Langford JI, Delhez R, de Keijser TH, Mittemeijer EJ. *J Appl Crystallogr* 1988;**41**: 173.
[14] Mhadhbi M, Khitouni M, Escoda L, Suñol JJ. *Materials Letters* 2010;**64**: 1802-1805.
[15] Valdrè G, Botton GA, Brown LM. *Acta Mater* 1999;**47**: 2303-2311.
[16] Bradley AJ, Jay AH. *Proc R Soc London, Ser A* 1932;**13**: 210.
[17] Ellner M. *Acta Crystallogr*, *Sec B Structural Science* 1995;**51**: 31.
[18] Zou Y, Saji S, Kusabiraki K. *MRS Res Bull* 2002;**37**: 123.
[19] Haghighi SE, Janghorban K, Izadi S. *J Alloys Compd* 2010;**495**: 260–264.
[20] Fu CL. *Phys Rev B* 1995;**52**: 3151–3180.
[21] Amils X, Nogues J, Surinach S, Baro MD. I*ntermetallics* 2000;**8**: 805–813.
[22] Askeland DR. *The Science and Engineering of Materials, 3rd ed, PWS Publishing Co.,Boston*; 1994.